PAPER • OPEN ACCESS

Emerging $(2+1)$D massive graviton in graphene-like systems

To cite this article: Patricio Salgado-Rebolledo and Jiannis K Pachos 2023 *New J. Phys.* **25** 033019

View the article online for updates and enhancements.

New Journal of Physics

The open access journal at the forefront of physics

PAPER

Emerging $(2+1)$D massive graviton in graphene-like systems

Patricio Salgado-Rebolledo[1,2,*] ⓘ and Jiannis K Pachos[3] ⓘ

[1] Université Libre de Bruxelles and International Solvay Institutes, ULB-Campus Plaine CP231, B-1050 Brussels, Belgium
[2] Institute of Theoretical Physics, Wrocław University of Science and Technology, Wrocław 50-370, Poland
[3] School of Physics and Astronomy, University of Leeds, Leeds LS2 9JT, United Kingdom
[*] Author to whom any correspondence should be addressed.

E-mail: patricio.salgado-rebolledo@pwr.edu.pl

Abstract

Unlike the fundamental forces of the Standard Model the quantum effects of gravity are still experimentally inaccessible. Rather surprisingly quantum aspects of gravity, such as massive gravitons, can emerge in experiments with fractional quantum Hall liquids. These liquids are analytically intractable and thus offer limited insight into the mechanism that gives rise to quantum gravity effects. To thoroughly understand this mechanism we employ a graphene-like system and we modify it appropriately in order to realise simple $(2+1)$-dimensional massive gravity model. More concretely, we employ $(2+1)$-dimensional Dirac fermions, emerging in the continuous limit of a fermionic honeycomb lattice, coupled to massive gravitons, simulated by bosonic modes positioned at the links of the lattice. The quantum character of gravity can be determined directly by measuring the correlations on the bosonic atoms or by the interactions they effectively induce on the fermions. The similarity of our approach to current optical lattice configurations suggests that quantum signatures of gravity can be simulated in the laboratory in the near future, thus providing a platform to address question on the unification theories, cosmology or the physics of black holes.

1. Introduction

An important open question in physics is that of observing quantum aspects of gravity. The coupling of gravity with matter is so weak that large, macroscopic masses are needed in order to generate an effect. Nevertheless, quantum effects are dominant in microscopic scales where gravity is negligible, thus, making quantum effects of gravity to be well beyond the reach of our current technology. This lack of any experimental evidence impedes our understanding of gravity at a fundamental level. For example, several often conflicting proposals exist for the quantisation of spacetime. Meanwhile, the $(3+1)$-dimensional graviton, the quantum particle that mediates gravity, is unrenormalisable, suffering from infinities in the theoretical level that cannot be removed. A possible way forward is to turn to condensed matter systems where gravitational effects could emerge at an effective level. As the couplings of such systems can be arbitrarily tuned then it would be possible to amplify the effect of geometric fluctuations in the simulated system and provide measurable signatures in proposed experiments.

The last decade has seen an increased interest in the geometric interpretation of condensed matter systems that emulate classical or quantum gravity effects. An interesting example is the emergence of massive gravitons in the ^{3}He-B superfluid [1], where gravity emerges from fermionic bilinears after symmetry breaking, in analogy with the massless emergent gravitational field proposed by Diakonov to construct a lattice-regularized quantum gravity theory [2]. Furthermore, of prominent interest is the exciting discovery that fractional quantum Hall liquids have collective excitations that are an analogue of gravitons. In particular, it has been demonstrated that the long wavelength limit of the Girvin-MacDonald-Platzman mode of the fractional quantum Hall effect [3, 4], also known as the *magnetoroton*, is properly described as a massive graviton excitation [5–7], which has been experimentally observed [8, 9]. Nevertheless, fractional

quantum Hall liquids are strongly interacting and thus analytically intractable. This intractability significantly limits our understanding of the mechanism responsible for the emergence of quantum gravity.

An alternative route is to engineer a system that effectively simulates quantum signatures of gravity. Such quantum simulations enable the realisation of a wide range of coupling regimes, thus enhancing properties that might be otherwise experimentally inaccessible. As an example, recent experimental advances in simulating quantum gauge theories offer insights into mechanisms that are not yet fully understood, like quark confinement [10]. Several platforms exist where classical gravity emerges. For example, it is possible to produce non-trivial extrinsic geometry by deforming the shape of graphene-like systems [11, 12] or to create tunnelling coupling inhomogeneities that generate intrinsic geometries [13, 14]. Unfortunately, simulations of quantum gravity have not been achieved so far. Roadblocks exist at the conceptual level, such as in realising quantum fluctuations of spacetime, as well as at the practical level, such as in engineering the complex self-interactions present in gravitational theories.

To resolve these problems we employ a simple and modular graphene-like system that can be analytically shown to give rise to massive gravitons in its low energy limit. In particular, we emulate Dirac fermions coupled to massive gravitons described by the Fierz–Pauli theory in 2+1 dimensions, which is known to posses two propagating degrees of freedom of helicity ± 2. To identify the right architecture we first consider the realisation of the Dirac field. We employ a two-dimensional honeycomb lattice configuration that describes $(2 + 1)$-dimensional Dirac fermions in its low energy limit. An effective background metric can be encoded in the couplings of the fermion lattice by making them position dependent [14]. Unlike extrinsically encoded geometry, which is hard to fluctuate, the intrinsically encoded one can be fluctuated by controlling the couplings of the model through auxiliary quantum fields [15]. In our system we employ bosonic modes positioned at the links of the lattice to induce fluctuations of the gravitational field. These modes are coupled to the fermionic ones and are subject to density-density self-interactions in a particular way that gives rise to a semiclassical expansion of $(2 + 1)$-dimensional massive gravitons coupled to Dirac fermions.

In recent years, $2 + 1$ dimensions have attracted great attention since they provide tractable models for gravity. Unlike $(3 + 1)$-dimensional gravity, pure $(2 + 1)$-dimensional Einstein gravity has no local propagating degrees of freedom and can be reformulated as a Chern–Simons theory [16, 17] with boundary degrees of freedom given in terms of two-dimensional conformal field theories [18–21]. A mass term in the Einstein–Hilbert action introduces local gravitational degrees of freedom that imprint their effects on the local properties of the Dirac fermions. In higher dimensions, adding a mass for the graviton has been considered as a possibility to resolve the cosmological constant problem, as well as in the construction of theories for dark matter [22]. In four dimensions, the first consistent theory of massive gravity free of Boulware-Deser ghosts was found by de Rham, Gabadaze and Tolley [23]. Subsequently, massive generalisations of the Einstein–Hilbert action in 2+1 dimensions have been explored such as Topologically Massive Gravity, New Massive Gravity and Zwei–Dreibein Gravity [24–26].

Apart from identifying a lattice model that effectively gives rise to massive gravitons in $2 + 1$ dimensions, our proposed architecture allows for quantum simulations with optical lattices. Ultra-cold atoms in optical lattices have proven to be an ideal system for probing interacting high-energy theoretical models or condensed matter physics that are otherwise inaccessible. From realising many-body localisation [27–30] and non-ergodicity in strongly correlated systems [31, 32] to simulating lattice gauge theories [10, 33–37] or probing topological phases [38–41], optical lattice technology is an invaluable component in advances of modern physics [42]. Such simulations keep the promise of realising lattice gauge theories that can be used to illustrate quark confinement, a fundamental phenomenon that still remains a mystery [43]. In particular, hexagonal optical lattices with fermionic or bosonic atoms have already been realised in the laboratory [40, 41]. Moreover, a shift in the paradigm of quantum simulations with cold atoms has happened with the suitable Yukawa-like coupling between fermionic and bosonic atoms for realising fluctuating gauge fields coupled to Dirac fermions [15] that lead to numerous advances towards the quantum simulation of gauge theories [33–37]. Here, we present a novel boson-fermion interaction that encodes fluctuating gravitational fields coupled to Dirac fermions. The final necessary ingredient is the realisation of bosonic self-interaction terms that give rise to dynamics of the gravitational field. Such terms can be realised by employing Feshbach resonances that are routinely employed in experiments to realise a wide range of interactions between bosonic atoms [44–47]. The Yukawa-like coupling between fermions and bosons causes the fermions to interact [48], an effect that can be experimentally witnessed in the fermionic correlators through the violation of Wick's theorem [49]. The components necessary for this simulation, such as 2D Dirac fermions, mixtures of bosonic and fermions optical lattices and for controlling atomic intra and inter-species interactions, are routinely implemented with current experiments. Hence, optical lattices offer a key tool towards realising quantum properties of gravity in the laboratory.

2. Dirac fermions coupled to gravitational fluctuations

We first present the $(2 + 1)$-dimensional gravitational theory that we want to simulate. We choose the simplest possible theory that has interesting dynamics. To begin with, we choose a torsionless theory where all the dynamics comes from curvature. Moreover, General Relativity in three spacetime dimensions is known for possessing only global or boundary degrees of freedom, while no local propagating modes exist in the bulk similar to the theory in four spacetime dimensions. An interesting generalisation of this theory at the linear level is obtained by adding the Fierz–Pauli mass term. By endowing gravitons with a mass, the theory acquires two propagating degrees of freedom. This is the model we simulate with our lattice simulator.

To obtain spacetime geometries that can be realised with optical lattices we consider the spacetime metric to be in Gaussian form. This form provides a separation of time from space, thus giving a time evolution of the gravitational system that looks similar to the time evolution of the optical lattice, as dictated by the Schrödinger equation. This condition corresponds to choosing the spacetime coordinates in such a way that the metric $g_{\mu\nu}$ looks like:

$$ds^2 = g_{\mu\nu}dx^\mu dx^\nu = -dt^2 + \left(l^2 \delta_{ij} + 8\pi G h_{ij}\right) dx^i dx^j, \tag{1}$$

where G is Newton's constant, l is a constant and $\mu = (t,i)$ denotes spacetime indices with $i = (x,y)$. To simplify the required optical lattice architecture we consider a gravity model where h_{ij} is diagonal. This considerably simplifies the constraint structure of the theory and avoids the need of introducing extra relations between the lattice variables in order to preserve the constraints during time evolution. The coupling of the gravitation field with the Dirac fermions is best described in terms of the dreibein field e^A_μ, given by $g_{\mu\nu} = \eta_{AB}e^A_\mu e^B_\nu$, where $A = (0, a = 1, 2)$ denotes Lorentz indices and $\eta = \text{diag}(-,+,+)$ is the metric of the local tangent Minkowski space. Parallel transport is then defined by the spin connection ω^A_μ satisfying $\partial_\mu e^A_\nu - \Gamma^\rho_{\mu\nu}e^A_\rho + \epsilon^A_{BC}\omega^B_\mu e^C_\nu = 0$, where $\Gamma^\rho_{\mu\nu}$ is the affine Christoffel connection. We consider gravitational fluctuations of a flat geometry, $\bar{e}^A_\mu$. In this case the fluctuating gravitational field translates into fluctuations of the dreibein, ξ^A_μ, and fluctuations of the spin connection, v^A_μ, of a flat background, i.e:

$$e^A_\mu = \bar{e}^A_\mu + 8\pi G \xi^A_\mu, \qquad \omega^A_\mu = 8\pi G v^A_\mu. \tag{2}$$

Spacetime geometries of the form given in (1), with h_{ij} diagonal, are described by:

$$\bar{e}^A_\mu = \begin{pmatrix} 1 & 0 \\ 0 & l\delta^a_i \end{pmatrix}, \quad \xi^A_\mu = \begin{pmatrix} 0 & 0 \\ 0 & \xi^a_i \end{pmatrix}, \quad \xi^a_i = \begin{pmatrix} \xi^1_x & 0 \\ 0 & \xi^2_y \end{pmatrix}, \tag{3}$$

where ξ^a_i's are the spatial dreibein fluctuations. The metric fluctuations are then given by $h_{ij} = l\left(\delta_{ai}\xi^a_j + \delta_{aj}\xi^a_i\right)$. Furthermore, we consider torsionless geometries, for which the spin connection perturbation v^A_μ can be expressed in terms of derivatives of ξ^A_μ (see appendix A for details).

In the following we consider a gravitational model described by the action:

$$S[\psi,\xi] = S_{\text{Dirac}}[\psi,\xi] + S_{\text{gr}}[\xi], \tag{4}$$

where S_{Dirac} is the action for a Dirac spinor ψ that includes the coupling of the geometry ξ^a_i to the fermionic current, whereas S_{gr} is a purely gravitational action that describes the spatial dreibein fluctuations ξ^a_i in a flat background geometry.

2.1. Fermionic action
The fermion action describes a massless Dirac field on curved space:

$$S_{\text{Dirac}} = \frac{i}{2} \int d^3x |e| \left(\bar{\psi} e^\mu_A \gamma^A \overrightarrow{D}_\mu \psi - \bar{\psi} \overleftarrow{D}_\mu e^\mu_A \gamma^A \psi \right), \tag{5}$$

where $\bar{\psi} = \psi^\dagger \gamma^0$, and the covariant derivative acting on fermionic fields is defined as $\overrightarrow{D}_\mu = \overrightarrow{\partial}_\mu + \omega_\mu$ and $\overleftarrow{D}_\mu = \overleftarrow{\partial}_\mu - \omega_\mu$ with $\omega_\mu = \frac{1}{4}\epsilon_{ABC}\omega^A_\mu \gamma^B \gamma^C$. In order to compare the fermionic action S_{Dirac} with the one coming from the optical lattice simulation, we rescale the corresponding spinor ψ as $\psi \longrightarrow \psi/\sqrt{|e|}$, so that they both satisfy flat anti-commutation relations [50]. Next we split the temporal and spatial indices and implement the semiclassical expansion (2). For small Newton's constant the resulting fermionic action to linear order in G is given by:

$$S_{\text{Dirac}}[\psi,\xi] = i \int d^3x \left[\bar{\psi}\gamma^0\dot{\psi} + \bar{\psi}\gamma^i\partial_i\psi \right] - \frac{8i\pi G}{l^2}\int d^3x \left[\xi_a^i\bar{\psi}\gamma^a\partial_i\psi + \frac{1}{2}\partial_i\xi_a^i\bar{\psi}\gamma^a\psi \right],$$ (6)

where we have defined the inverse field $\xi_a^i = \delta_b^i\delta_j^a\xi_j^b$.

2.2. Gravitational action

In order to describe the dynamics of the gravitational field we start with the Palatini action for e^A and ω^A given by:

$$S_{\text{gr}} = \frac{1}{8\pi G}\int d^3x \epsilon^{\mu\nu\rho}e_\mu^A\left(\partial_\nu\omega_{A\rho} + \frac{1}{2}\epsilon_{ABC}\omega_\nu^B\omega_\rho^C\right).$$ (7)

As before, we consider the semiclassical expansion of S_{gr} with zero torsion and background curvature. The dominant order in the G expansion is then given by the massless Fierz–Pauli action for $h_{\mu\nu} = \bar{e}_{A\mu}\xi_\nu^A + \bar{e}_{A\nu}\xi_\mu^A$ (see appendix B for details). The particular action and geometries are suitably chosen so that the resulting Hamiltonian can be directly modelled with ultra-cold atoms in optical lattices. Moreover, considering a metric in Gaussian coordinates (1) is convenient at the quantum level, since it allows to eliminate the so-called *conformal divergences* in the graviton path integral [51].

    The action (7) describes a topological theory with no propagating degrees of freedom. In order to have local degrees of freedom, akin to $(3+1)$-dimensional General Relativity, we introduce a mass term for the gravitational field. Here, we consider massive gravitons ξ_μ^A described by the Fierz–Pauli theory [52], obtained by adding the mass term:

$$4\pi G\mu^2\epsilon^{\mu\nu\rho}\epsilon_{ABC}\bar{e}_\mu^A\xi_\nu^B\xi_\rho^C,$$ (8)

in the Lagrangian (7) after linearisation. Combining (2), (7) and (8) finally gives (see appendix B for details):

$$S_{\text{gr}}[\xi] = -4\pi G\int d^3x \epsilon^{ij}\epsilon_{ab}\left(\dot{\xi}_i^a\dot{\xi}_j^b - \mu^2\xi_i^a\xi_j^b\right),$$ (9)

which is the effective massive gravitational action, with ξ_i^a given by (3). Note that we have introduced the mass term (8) by hand. It is known that the Fierz–Pauli action in 2+1 dimensions can be obtained from New Massive Gravity [25, 53], a full gravitational theory with quadratic-in-curvature terms that possesses two local propagating degrees of freedom of helicity ±2. Alternatively, a different gravitational theory, whose weak field limit leads to the same massive Fierz–Pauli action has been proposed in [54].

2.3. Total Hamiltonian

In order to determine the optical lattice configuration required to simulate this gravity model, we need first to obtain its Hamiltonian. The Hamiltonian corresponding to the action (4) is given by (for details, see appendix C):

$$H = \int d^2x \left[\psi^\dagger h(\boldsymbol{p})\psi + \mathcal{H}_{\text{gr}} \right],$$ (10)

where the single particle Hamiltonian $h(\boldsymbol{p})$ reads:

$$h(\boldsymbol{p}) = \frac{\gamma^0}{l}\left(\delta_a^i\gamma^a - \frac{8\pi G}{l}\xi_a^i\gamma^a\right)(-i\partial_i) + \frac{4i\pi G}{l^2}\partial_i\xi_a^i\gamma^0\gamma^a,$$ (11)

and the gravitational Hamiltonian $\mathcal{H}_{\text{gr}}$ equals:

$$\mathcal{H}_{\text{gr}} = -\frac{1}{16\pi G}\epsilon_{ij}\epsilon^{ab}\pi_a^i\pi_b^j + 4\pi G\mu^2\epsilon^{ij}\epsilon_{ab}\xi_i^a\xi_j^b.$$ (12)

Here $\pi_a^i = \text{diag}(\pi_1^x, \pi_2^y)$ is the canonical momentum conjugate to ξ_i^a given in (3). The geometric fluctuations and their conjugate momenta can be expressed as:

$$\xi_x^1 = \frac{1}{\sqrt{2}}(q_1^\dagger + q_1), \qquad \pi_1^x = -\frac{i}{\sqrt{2}}(q_1^\dagger - q_1),$$

$$\xi_y^2 = \frac{1}{\sqrt{2}}(q_2^\dagger + q_2), \qquad \pi_2^y = -\frac{i}{\sqrt{2}}(q_2^\dagger - q_2),$$ (13)

where the operators q_a and $q_a^\dagger$ ($a = 1, 2$) satisfy the bosonic commutation relations $[q_a(x), q_b^\dagger(y)] = \delta_{ab}\delta^{(2)}(x-y)$ and $[q_a(x), q_b(y)] = 0 = [q_a^\dagger(x), q_b^\dagger(y)]$. It is in terms of these quantum operators that we can establish a map between (10) and an optical lattice Hamiltonian.

3. Optical lattice simulator

We now design an optical lattice configuration that simulates the quantum gravity model given by (10) in its low energy limit. We first present a configuration that gives rise to Dirac fermions in a fixed background geometry encoded in the tunnelling couplings of the lattice [14]. Then we introduce link quantum variables d_m ($m = x, z$) that fluctuate this geometry. Consider a two-dimensional optical lattice with honeycomb configuration where fermionic atoms, a and b, live at its vertices, as shown in figure 1(Left). The fermions are subject to the tunnelling Hamiltonian:

$$H_{\text{latt}} = \sum_{\boldsymbol{i}} \left[J_x(\boldsymbol{i}) a_{\boldsymbol{i}}^\dagger b_{\boldsymbol{i}+\boldsymbol{n}_1} + J_y(\boldsymbol{i}) a_{\boldsymbol{i}}^\dagger b_{\boldsymbol{i}+\boldsymbol{n}_2} + J_z(\boldsymbol{i}) a_{\boldsymbol{i}}^\dagger b_{\boldsymbol{i}} \right] + \text{h.c.}, \tag{14}$$

where $\boldsymbol{i} = (i_x, i_y)$ gives the position of unit cells on the lattice, the couplings of the first two terms are equal ($J_x = J_y$), and both J_x and J_z are in general position dependent. At half-filling, the low energy sector of the model is described by the Dirac Hamiltonian $H_{\text{latt}} \approx \int d^2x\, \psi^\dagger\, \tilde{h}(\boldsymbol{p})\, \psi$ [14] with (see appendix D for details):

$$\tilde{h}(\boldsymbol{p}) = -\frac{\sqrt{3}i}{2} \sqrt{4J_x^2 - J_z^2}\, \gamma^0 \gamma^1 \partial_x - \frac{3i}{2} J_z \gamma^0 \gamma^2 \partial_y + \frac{\sqrt{3}i}{2} \partial_x \left(\sqrt{4J_x^2 - J_z^2} \right) \gamma^0 \gamma^1 + \frac{3i}{2} \partial_y J_z \gamma^0 \gamma^2. \tag{15}$$

The coefficients of $\gamma^0 \gamma^1 (-i\partial_x)$ and $\gamma^0 \gamma^2 (-i\partial_y)$ play the role of the diagonal space components of the dreibein, e_x^1 and e_y^2, respectively, as shown in figure 1(Right). To introduce quantum fluctuations in the J couplings, and thus in the corresponding dreibeins, we insert bosonic modes α_x and α_z at the edges of the lattice, as shown in figure 1(Left). To realise this configuration of atomic boson-fermion mixture we need two pairs of triangular lattices, one fermionic and one bosonic, as shown in figure 2. Triangular lattices can routinely be created in the laboratory for bosonic [55] and fermionic [56] atoms. Optical lattices with interacting mixtures of bosonic and fermionic atoms have been realised and their rich physics has been extensively investigated [57–59].

When the bosonic and fermionic lattices shown in figure 2 are superposed, the bosonic modes α_x and α_z control the tunnelling of fermions from site $\boldsymbol{i}$ to site $\boldsymbol{k}$ in the $m(= x, z)$ direction, through the interaction $\Delta_m \alpha_m^\dagger \alpha_m a_{\boldsymbol{i}}^\dagger b_{\boldsymbol{k}}$ [15]. We take the α_m modes to correspond to a bosonic condensation with particle density D_m and quantum fluctuations d_m, i.e:

$$\alpha_m(\boldsymbol{i}) = D_m(\boldsymbol{i}) + d_m(\boldsymbol{i}), \tag{16}$$

where $[d_m(\boldsymbol{i}), d_m^\dagger(\boldsymbol{j})] = \delta_{\boldsymbol{ij}}$, for $m = x, z$. In the weak fluctuation limit $\langle d_m^\dagger d_m \rangle \ll D_m^2$, the interactions between bosons and fermions give rise to tunnelling couplings of the form $J_m = \Delta_m D_m (D_m + d_m^\dagger + d_m)$. If we choose the optical lattice parameters as:

$$D_x = \sqrt{2} D_z = -\frac{l}{4\pi G}, \qquad \Delta_x = \frac{\Delta_z}{2} = \frac{32\pi^2 G^2}{3l^3}, \tag{17}$$

with the operator redefinition $q_1 = 2\sqrt{2} d_x/3 - d_z/3$ and $q_2 = d_z$ that preserves bosonic commutation relations, we find that, to linear order in G, the optical lattice Hamiltonian (14) is mapped to the field theory one (11) (for details, see appendices C and D). Constant tunnelling terms can be added in (14) to arbitrarily tune the values of the densities D_m.

The self-interaction terms (12) of the gravitational Hamiltonian can be obtained from the following purely bosonic interactions:

$$\begin{aligned}
\mathcal{H}_{\text{boson}} = {}& \frac{1}{24\pi G} (\alpha_z^\dagger - \alpha_z) \left(\sqrt{2}(\alpha_x^\dagger - \alpha_x) - \frac{1}{2}(\alpha_z^\dagger - \alpha_z) \right) + \frac{8\pi G\mu^2}{3} \left(\alpha_z^\dagger \alpha_z + \alpha_x^\dagger \alpha_x \right) \\
& - \frac{256\pi^3 G^3 \mu^2}{3l^2} \alpha_z^\dagger \alpha_z \left(\alpha_x^\dagger \alpha_x - \frac{1}{2} \alpha_z^\dagger \alpha_z \right),
\end{aligned} \tag{18}$$

restricted to the weak fluctuation regime of α_m.

Figure 1. (Left) The optical lattice configuration with fermionic and bosonic atoms. The unit cell of the honeycomb lattice (dashed box) comprises two fermionic modes a and b. The fermionic atoms tunnel along the three different directions of th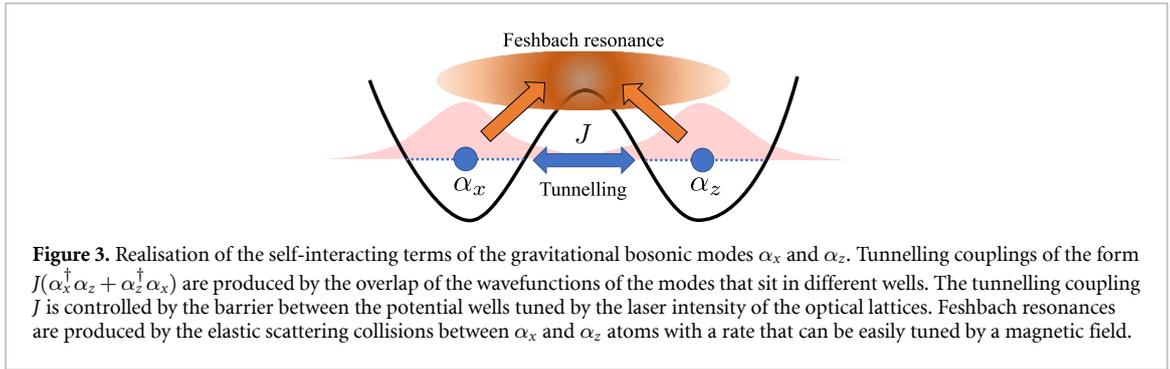e trivalence lattice with couplings J_x, $J_y(=J_x)$, and J_z. The vectors $\boldsymbol{n}_1 = (\sqrt{3}/2, 3/2)$ and $\boldsymbol{n}_2 = (-\sqrt{3}/2, 3/2)$ transport between different unit cells. (Right) In the low energy limit the dispersion relation $E(\boldsymbol{p})$ of the fermions is given by Dirac cones. Non-equal tunnelling couplings, J_x and J_z, cause the Dirac cone to be deformed, with its geometry encoded in the dreibein components e_x^1 and e_y^2, effectively describing background gravity. Bosonic modes α_x and α_z, describing Bose–Einstein condensates, are inserted that control the fermionic tunnelling couplings with their populations. Fluctuations of the condensates simulate fluctuations in e_x^1 and e_y^2, i.e. gravitational fluctuations.

Figure 2. The optical lattice configuration of figure 1 is obtained by superposing two pairs of triangular lattices, a fermionic pair (Left) and a bosonic pair (Right). The pair of lattices that hosts fermionic modes a and b gives rise to the honeycomb lattice model when nearest neighbour tunnelling couplings are activated. The pair of bosonic lattice modes, α_x and α_z, is positioned at the links of the honeycomb lattice. The x-confinement of the α_x modes is made weaker to overlap with both J_x and J_y links of the honeycomb lattice (see figure 1). By activating interactions between the bosonic and fermionic atoms, $\Delta_m \alpha_m^\dagger \alpha_m a_i^\dagger b_{\boldsymbol{k}}$, the population of the bosonic modes at site m controls the fermionic tunnelling between sites $\boldsymbol{i}$ and $\boldsymbol{k}$, thus giving rise to the effective interaction between Dirac fields and fluctuating geometry.

3.1. Realisation of interactions

The quantum simulation of Dirac fermions coupled to fluctuating gravity requires the realisation of (10) with the fermionic part coupled to the bosons given by (11) and the self-interactions of bosons (18). The first component is the realisation of the $(2+1)$-dimensional Dirac dispersion relation of the form (15). This has already been achieved in the laboratory with ultracold fermionic atoms by several experimental groups [60–62]. Of much interest is the possibility the optical lattices offer in running the couplings at will thus allowing the effective encoding of background geometry [14]. Introducing fluctuations in the background geometry can be achieved with optical lattices by coupling bosonic and fermionic species together, as shown in figure 1(Left). This method is similar to the minimal coupling realisation with optical lattices [15], suitably adapted here to encode the coupling between Dirac fermions and dreibeins. It incorporates Bose–Einstein condensates with weak boson number fluctuations. When positioned at the links of the honeycomb lattice they couple with the tunnelling fermions producing the desired boson-fermion couplings dictated by (11). Note that the tunnelling couplings of fermions, J_x, J_y and J_z, and the condensation particle densities D_m can be routinely tuned and controlled in an experiment by controlling the laser intensity of the optical lattices and the frequency of the magnetic or optical trapping of the condensate, respectively.

The final ingredient is the realisation of the gravitational self-interacting terms presented in (18). This Hamiltonian includes chemical potentials as well as tunnelling, pairing and interacting terms between the α_m bosonic atoms. Chemical potentials can be easily tuned with great accuracy by controlling the populations or the trapping potential of the cold atoms. Tunnelling terms between two different bosonic modes, such as α_x and α_z, can be obtained by changing the potential barrier between the corresponding sites, as shown in figure 3. These bosonic terms can be controlled independently from the fermionic atoms as they are created by independent optical lattices (see appendix E for details). Pairing terms of the form $\alpha_z^\dagger \alpha_x^\dagger + \alpha_z \alpha_x$ can be activated by resonances to molecular bound states as it has been recently demonstrated with homonuclear

Figure 3. Realisation of the self-interacting terms of the gravitational bosonic modes α_x and α_z. Tunnelling couplings of the form $J(\alpha_x^\dagger \alpha_z + \alpha_z^\dagger \alpha_x)$ are produced by the overlap of the wavefunctions of the modes that sit in different wells. The tunnelling coupling J is controlled by the barrier between the potential wells tuned by the laser intensity of the optical lattices. Feshbach resonances are produced by the elastic scattering collisions between α_x and α_z atoms with a rate that can be easily tuned by a magnetic field.

^{39}K-^{39}K or heteronuclear ^{41}K-^{87}Rb mixtures [46, 47]. Population interactions of the form $\alpha_z^\dagger \alpha_z \alpha_x^\dagger \alpha_x$ can be accurately controlled by employing Feshbach resonances, e.g. between Rb atoms, as has already been demonstrated experimentally [44, 45] (see figure 3). Such resonances are very versatile as they can generate positive, negative or zero interactions, or change the collision rate by several orders of magnitude just by selecting appropriate atomic states and tuning appropriately the external magnetic field. Hence, it is plausible that the quantum gravity model coupled to Dirac fermions given in (10) can be experimentally realised with a mixture of bosonic and fermionic ultra-cold atoms in optical lattices.

4. Quantum signatures of gravity

The optical lattice system given by (14) and (18) in the low energy limit simulates Dirac fermions coupled to massive gravitons (10). The presence of simulated quantum effects of gravity can be witnessed by directly measuring the bosonic field or by measuring the effect it has on the fermionic field. The pure gravity Hamiltonian (12) describes simple tunnelling and pairing terms between bosonic modes 1 and 2. The signatures of these couplings can be directly measured in the quantum correlations $\langle d_1^\dagger d_2^\dagger \rangle$ and $\langle d_1^\dagger d_2 \rangle$ of the corresponding Bose-Einstein condensates [63]. We can establish how faithfully the simulating Hamiltonian (18) reproduces the desired gravitational Hamiltonian (12) by determining the dependence of the correlations on the 'gravitational' coupling G.

We present now how to identify the presence of a fluctuating gravitational field from the behaviour of the fermionic quantum correlations. In the absence of gravity, i.e. $G = 0$, the interaction term of the Dirac field disappears giving rise to free fermions. If the fermions are coupled to a fluctuating gravitation field then interactions between them emerge. Hence, we can identify the presence of fluctuating geometry by identifying if the Dirac fermions are free or interacting. The distinction between the two can happen by testing the applicability of Wick's theorem, i.e. testing the decomposition of four-point quantum correlations in terms of two-point correlations. Such two- and four-point correlation measurements are routinely realised in cold atom experiments. Hence, our scheme provides a direct quantum signature of gravity in terms of experimentally feasible components.

The partition function of the system at temperature T is given by:

$$Z = \int \mathcal{D}\xi \, \mathcal{D}\pi \, \mathcal{D}\psi \, \mathcal{D}\bar\psi \, \exp\left(-\frac{1}{k_B T} \int \mathrm{d}^2 x \, \mathcal{H}\right), \tag{19}$$

where $\mathcal{H} = \psi^\dagger \, h(\boldsymbol{p}) \, \psi + \mathcal{H}_{\mathrm{gr}}$ and k_B is the Boltzmann constant. To determine the behaviour of the fermions due to their interactions mediated by gravitational fluctuations we can integrate the bosonic part, i.e. ξ and π, of (19) and derive the effective fermionic Hamiltonian. Integrating out the momenta, π_a^i, leads to an irrelevant global factor in Z. We can subsequently integrate out the bosonic field ξ_i^a, which up to an overall constant yields:

$$Z = \int \mathcal{D}\psi \, \mathcal{D}\bar\psi \, \exp\left(-\frac{1}{k_B T} \int \mathrm{d}^2 x \, \mathcal{H}_{\mathrm{eff}}\right), \tag{20}$$

with the effective Hamiltonian:

$$\mathcal{H}_{\mathrm{eff}} = -i\bar\psi \, \gamma^i \, \partial_i \psi - \frac{4\pi \, G}{l^2 \mu^2} \epsilon_{ab} \epsilon^{ij} \mathcal{J}_i^a \mathcal{J}_j^b, \tag{21}$$

where $\mathcal{J}_i^a = \frac{i}{2l} \left(\bar\psi \gamma^a \partial_i \psi - \partial_i \bar\psi \gamma^a \psi \right)$ is the fermionic current. As a result the partition function of the system is Hubbard-like, effectively describing interacting fermions with a coupling proportional to the gravitational

constant G. The presence of such attractive fermion interactions can be measured in optical lattices by monitoring its Hubbard-like behaviour [64]. It is interesting to note that similarity of the interaction term in (21) and the effective gravitational models considered in [1, 2].

An alternative manifestation of interactions (21) mediated by the gravitational field is on the fermionic correlations, which can be witnessed by testing the applicability of Wick's theorem. In the absence of gravitational fluctuations, i.e. for Newton's constant $G \to 0$ in (2) or for fluctuations $\xi_i^a \to 0$, the effective partition function corresponds to free fermions, as seen by (21). For this case, Wick's theorem states that all four-point quantum correlators of the ground state can be exactly decomposed in terms of two-point correlators. Such four-point correlators of fermions can be expressed in terms of fermionic densities and two-point correlations and thus can be directly measured in cold atom experiments [42]. When the interactions induced by the gravitational field are present, i.e. for $G \neq 0$, Wick's decomposition does not apply, leaving a difference that can be determined by measurements of fermionic correlations [49]. In the perturbative regime considered here this difference gives a measure of the coupling G between the Dirac fermions and the gravitational field.

5. Conclusions

Among the forces of nature gravity keeps its quantum aspects well hidden. This lack of experiential evidence hinders the theoretical understanding of quantum gravity and its unification with the rest of the fundamental forces within the Standard Model. Here we propose a way of simulating quantum signatures of massive gravity coupled to Dirac fermions in the laboratory. By building upon recent methods, developed for simulating scalar or gauge fields coupled to Dirac fermions, we are able to model Dirac fermions in the presence of fluctuating geometries, which is a unique characteristic of quantum gravity. This breakthrough was possible by encoding spacetime geometries intrinsically in the couplings of the system and then employing bosonic fields that fluctuate these couplings. The bosonic fields are appropriately designed in order to give rise to a massive quantum graviton akin to the magnetoroton emerging in fractional quantum Hall liquids. As our model provides a direct link between microscopic system components and properties of the effective massive gravity, it sheds light into the mechanism behind the emergence of quantum gravitons in strongly interacting systems.

Beyond providing an example where massive gravitons emerge in a condensed matter system, our model can be simulated with optical lattices. The components used in our proposal, such as the fermionic honeycomb lattice or the bosonic condensates, can be realised in the laboratory with current ultra-cold atom technology. Quantum signatures of the emerging geometry can be witnessed in the effective fermionic interactions mediated by their coupling to fluctuating geometry, which can be directly probed in optical lattice experiments.

Our work opens up a host of various applications. It is intriguing to consider the behaviour of various quantum gravity and cosmology theories in $1 + 1$, $2 + 1$ or $3 + 1$ dimensions with or without fermions. Several open questions exist about the quantum aspects of gravity, cosmology and the physics of black holes that can be addressed within the framework presented here. We envision that our proposal will initiate a new line of investigations where interacting models that simulate gravity can be realised in the laboratory and guide theoretical investigations towards the understanding of quantum aspects of gravity in nature.

Data availability statement

The data that support the findings of this study are available upon reasonable request from the authors.

Acknowledgment

Appendix A. Spin connection

We consider a three-dimensional geometry whose metric tensor is defined by a set of dreibeins e_μ^A:

$$g_{\mu\nu} = \eta_{AB} e_\mu^A e_\nu^B. \tag{A1}$$

where here $A = (0, a = 1, 2)$ denotes Lorentz indices, $\mu = (t, i = x, y)$ stand for manifold indices, and $\eta = \text{diag}(-, +, +)$ is the Minkowski metric. Parallel transport is defined by the spin connection ω_μ^A, which can be obtained from the vielbein postulate:

$$\partial_\mu e_\nu^A - \Gamma_{\mu\nu}^\rho e_\rho^A + \epsilon_{BC}^A \omega_\mu^B e_\nu^C = 0, \tag{A2}$$

where $\Gamma_{\mu\nu}^\rho$ is the affine Christoffel connection and ϵ^{ABC} the Levi-Civita symbol ($\epsilon^{012} = 1$). In this case, the gravitational fluctuations translate into fluctuations of the dreibein and the spin connection:

$$e_\mu^A = \bar{e}_\mu^A + \frac{1}{8\pi G}\xi_\mu^A, \qquad \omega_\mu^A = \bar{\omega}_\mu^A + \frac{1}{8\pi G}v_\mu^A. \tag{A3}$$

We restrict the analysis to flat backgrounds with constant dreibein and vanishing spin connection. Therefore we set:

$$\bar{e}_\mu^A = \text{constant}, \qquad \bar{\omega}_\mu^A = 0. \tag{A4}$$

Furthermore, we consider torsionless geometries. In this case taking the antisymmetric part of (A2) allows one to express ω_μ^A in terms the dreibein and its derivatives. For the corresponding perturbations (A3) one finds the relation:

$$\epsilon^{\mu\nu\rho}\left(\partial_\nu \xi_\rho^A + \epsilon_{BC}^A \bar{e}_\nu^B v_\rho^C\right) = 0, \tag{A5}$$

which can be used to find the form of the spin connection perturbations v_μ^A:

$$v_\mu^A = M_{\mu\nu}^{AB}\epsilon^{\nu\alpha\beta}\partial_\alpha \xi_{B\beta}, \quad M_{\mu\nu}^{AB} \equiv \frac{1}{\bar{e}}\left(\frac{1}{2}\bar{e}_\mu^A \bar{e}_\nu^B - \bar{e}_\nu^A \bar{e}_\mu^B\right), \tag{A6}$$

where $\bar{e} = \det(\bar{e}_\mu^A)$. When restricted to metrics of the form (1), which means:

$$\bar{e}_\mu^A = \begin{pmatrix} 1 & 0 \\ 0 & \bar{e}_i^a \end{pmatrix}, \qquad \xi_\mu^a = \begin{pmatrix} 0 & 0 \\ 0 & \xi_i^a \end{pmatrix}, \tag{A7}$$

the components of the spin connection reduce to:

$$v_t^0 = -\frac{4\pi G}{\bar{e}}\epsilon^{ij}\bar{e}_i^a \dot{\xi}_{aj}, \qquad v_i^0 = -\frac{8\pi G}{\bar{e}}\epsilon^{jk}\bar{e}_i^a \partial_j \xi_{ak}, \qquad v_t^a = 0, \qquad v_i^a = 8\pi G M_{ij}^{ab}\epsilon^{jk}\dot{\xi}_{bk}. \tag{A8}$$

Appendix B. Gravity action

In order to describe gravitational fluctuations, we start with the Palatini action for e_μ^A and ω_μ^A:

$$S_{\text{gr}} = \frac{1}{8\pi G}\int d^3 x \epsilon^{\mu\nu\rho} e_\mu^A \left(\partial_\nu \omega_{A\rho} + \frac{1}{2}\epsilon_{ABC}\omega_\nu^B \omega_\nu^C\right). \tag{B1}$$

Using (A3), the action can be expanded in powers of the $(2+1)$-dimensional reduced Planck mass $1/8\pi G$ as:

$$S_{\text{gr}}[\xi] = \frac{1}{8\pi G}S_{\text{gr}}^{(0)} + S_{\text{gr}}^{(1)} + 8\pi G S_{\text{gr}}^{(2)}. \tag{B2}$$

Defining the background curvature and torsion,

$$\bar{R}_{\mu\nu}^A = \partial_{[\mu}\bar{\omega}_{\nu]}^A + \frac{1}{2}\epsilon_{BC}^A \bar{\omega}_{[\mu}^B \bar{\omega}_{\nu]}^C = 0,$$
$$\bar{T}_{\mu\nu}^A = \partial_{[\mu}\bar{e}_{\nu]}^A + \epsilon_{BC}^A \bar{\omega}_{[\mu}^B \bar{e}_{\nu]}^C = 0, \tag{B3}$$

the different terms in the action (B2) can be written as:

$$S_{\text{gr}}^{(0)} = \frac{1}{2}\int d^3 x \epsilon^{\mu\nu\rho}\bar{e}_\mu^A \bar{R}_{A\nu\rho},$$
$$S_{\text{gr}}^{(1)} = \frac{1}{2}\int d^3 x \epsilon^{\mu\nu\rho}\left(\xi_\mu^A \bar{R}_{A\nu\rho}, + \bar{v}_\mu^A \bar{T}_{A\nu\rho}\right),$$
$$S_{\text{gr}}^{(2)} = \int d^3 x \epsilon^{\mu\nu\rho}\left(\xi_\mu^A \bar{D}_\nu v_{A\rho} + \frac{1}{2}\epsilon_{ABC}\bar{e}_\mu^A v_\nu^B v_\rho^C\right). \tag{B4}$$

Considering a flat torsionless background implies that $\bar{R}^A_{\mu\nu} = 0 = \bar{T}^A_{\mu\nu}$. Replacing (A6) in (B4) and using tensor notation then yields:

$$S_{\mathrm{gr}}[\xi] = -4\pi G \int \mathrm{d}^3 x M^{AB}_{\mu\nu} \epsilon^{\mu\alpha\beta} \epsilon^{\nu\gamma\delta} \partial_\alpha \xi_{A\beta} \partial_\gamma \xi_{B\delta}. \tag{B5}$$

One can check that the action (B5) boils down to the massless Fierz–Pauli action for $h_{\mu\nu} = \bar{e}_{A\mu}\xi^A_\nu + \bar{e}_{A\nu}\xi^A_\mu$.

We are interesting in adding a mass μ to the geometry fluctuations ξ^A_μ. We do so by means of the Fierz–Pauli mass term:

$$4\pi G\mu^2 \epsilon^{\mu\nu\rho} \epsilon_{ABC} \bar{e}^A_\mu \xi^B_\nu \xi^C_\rho. \tag{B6}$$

Thus, implementing (A7) and (A8) in (B5) and adding the term (B6) restricted to those conditions, we find the following effective massive gravitational action:

$$S_{\mathrm{gr}}[\xi] = -4\pi G \int \mathrm{d}^3 x \epsilon^{ij} \epsilon_{ab} \left(\dot{\xi}^a_i \dot{\xi}^b_j - \mu^2 \xi^a_i \xi^b_j \right). \tag{B7}$$

where we have defined $\epsilon^{ij} \equiv \epsilon^{0ij}$.

Appendix C. Field theory Hamiltonian

The Hamiltonian density associated to the Lagrangian in (4) is obtained after a straightforward Legendre transformation:

$$\mathcal{H} = \Pi^\dagger \dot{\psi} + \dot{\psi} \Pi + \pi^i_a \dot{\xi}^a_i - \mathcal{L}, \tag{C1}$$

where the canonical momenta read:

$$\Pi^\dagger = \frac{\partial \mathcal{L}}{\partial \dot{\psi}} = i\psi^\dagger, \qquad \Pi = \frac{\partial \mathcal{L}}{\partial \dot{\psi}^\dagger} = 0,$$
$$\pi^i_a = \frac{\partial \mathcal{L}}{\partial \dot{\xi}^a_i} = -8\pi G \epsilon^{ij} \epsilon_{ab} \dot{\xi}^b_j, \tag{C2}$$

and satisfy the Poisson brackets:

$$\left\{ \psi_\alpha(x), \Pi^\dagger_\beta(y) \right\} = \left\{ \psi^\dagger_\alpha(x), \Pi_\beta(y) \right\} = -\delta_{\alpha\beta} \delta^{(2)}(x-y),$$
$$\left\{ \xi^a_i(x), \pi^j_b(y) \right\} = \delta^a_b \delta^j_i \delta^{(2)}(x-y). \tag{C3}$$

The Hamiltonian reduces to:

$$H = \int \mathrm{d}^2 x \, \mathcal{H} = \int \mathrm{d}^2 x \left[\psi^\dagger h(\boldsymbol{p}) \psi + \mathcal{H}_{\mathrm{gr}} \right], \tag{C4}$$

with the single particle hamiltonian $h(\boldsymbol{p})$:

$$h(\boldsymbol{p}) = \frac{\gamma^0}{l} \left(\delta^i_a \gamma^a - \frac{8\pi G}{l} \xi^i_a \gamma^a \right) (-i\partial_i) + \frac{4i\pi G}{l^2} \partial_i \xi^i_a \gamma^0 \gamma^a, \tag{C5}$$

and the gravitational Hamiltonian $\mathcal{H}_{\mathrm{gr}}$ given by:

$$\mathcal{H}_{\mathrm{gr}} = -\frac{1}{16\pi G} \epsilon_{ij} \epsilon^{ab} \pi^i_a \pi^j_b - 4\pi G\mu^2 \epsilon^{ij} \epsilon_{ab} \xi^a_i \xi^b_j. \tag{C6}$$

Since our analysis considers geometry fluctuations ξ^a_i that are diagonal, we define quantum operators of the form:

$$\xi^a_i = \begin{pmatrix} \xi^1_x & 0 \\ 0 & \xi^2_y \end{pmatrix}, \qquad \xi^1_x = \frac{1}{\sqrt{2}}(q^\dagger_1 + q_1), \qquad \xi^2_y = \frac{1}{\sqrt{2}}(q^\dagger_2 + q_2), \tag{C7}$$

where the operators $q_a, a = 1, 2$ satisfy the commutation relations:

$$[q_a(x), q^\dagger_b(y)] = \delta_{ab} \delta^{(2)}(x-y),$$
$$[q_a(x), q_b(y)] = 0 = [q^\dagger_a(x), q^\dagger_b(y)]. \tag{C8}$$

Thus, the canonical Poisson brackets (C3) are promoted commutators $\{\ ,\ \} \to -i[\ \ ]$, which then fixes the form of the momenta ξ_a^i to be:

$$\pi_a^i = \begin{pmatrix} \pi_1^x & 0 \\ 0 & \pi_2^y \end{pmatrix}, \qquad \pi_1^x = -\frac{i}{\sqrt{2}}(q_1^\dagger - q_1), \qquad \pi_2^y = -\frac{i}{\sqrt{2}}(q_2^\dagger - q_2). \tag{C9}$$

The flat background spatial metric is taken as $g_{ij} = l^2 \delta_{ij}$ with l an arbitrary constant, which implies:

$$\bar{e}_i^a = l\delta_i^a, \qquad \bar{e}_a^i = \frac{1}{l}\delta_a^i, \tag{C10}$$

and thus the gamma matrices on this background geometry reduce to:

$$\gamma^t = \gamma^0, \quad \gamma^i = \frac{1}{l}\delta_a^i \gamma^a. \tag{C11}$$

From this expressions we see that the single particle Hamiltlonian (C5) can be written as:

$$h(\boldsymbol{p}) = \left(\frac{1}{l} - \frac{4\sqrt{2}\pi G}{l^2}(q_1^\dagger + q_1)\right)\gamma^0\gamma^1(-i\partial_x) + \left(\frac{1}{l} - \frac{4\sqrt{2}\pi G}{l^2}(q_2^\dagger + q_2)\right)\gamma^0\gamma^2(-i\partial_y)$$
$$+ \frac{2\sqrt{2}i\pi G}{l^2}\left(\partial_x(q_1^\dagger + q_1)\gamma^0\gamma^1 + \partial_y(q_2^\dagger + q_2)\gamma^0\gamma^2\right), \tag{C12}$$

whereas the gravitational Hamiltonian (C6) takes the form:

$$\mathcal{H}_{\mathrm{gr}} = \frac{1}{16\pi G}(q_1^\dagger - q_1)(q_2^\dagger - q_2) - 4\pi G\mu^2(q_1^\dagger + q_1)(q_2^\dagger + q_2). \tag{C13}$$

In the following, we show how to translate (C4) into an optical lattice Hamiltonian.

Appendix D. Optical lattice Hamiltonian

We start considering an optical lattice with unequal tunnelling couplings:

$$H_{\mathrm{latt}} = \sum_{\boldsymbol{i}}\left(J_x a_{\boldsymbol{i}}^\dagger b_{\boldsymbol{i}+\boldsymbol{n}_1} + J_y a_{\boldsymbol{i}}^\dagger b_{\boldsymbol{i}+\boldsymbol{n}_2} + J_z a_{\boldsymbol{i}}^\dagger b_{\boldsymbol{i}}\right) + \mathrm{h.c.}, \tag{D1}$$

where $\boldsymbol{i} = (i_x, i_y)$ denotes the position of the unit cells (see figure 1). Expanding the operators in Fourier modes and defining:

$$\psi_{\boldsymbol{k}} = \begin{pmatrix} a_{\boldsymbol{k}} \\ b_{\boldsymbol{k}} \end{pmatrix}, \quad \tilde{h}(\boldsymbol{k}) = \begin{pmatrix} 0 & f(\boldsymbol{k}) \\ f^*(\boldsymbol{k}) & 0 \end{pmatrix}, \tag{D2}$$

where $f(\boldsymbol{k}) = J_x e^{-i\boldsymbol{k}\cdot\boldsymbol{n}_1} + J_y e^{-i\boldsymbol{k}\cdot\boldsymbol{n}_2} + J_z$, we find:

$$H_{\mathrm{latt}} = \sum_{\boldsymbol{k}} \psi_{\boldsymbol{k}}^\dagger \tilde{h}(\boldsymbol{k})\psi_{\boldsymbol{k}}. \tag{D3}$$

We consider the special case $J_x = J_y$. The Fermi points, $\boldsymbol{P}_\pm$, are defined by:

$$f(\boldsymbol{P}_\pm) = 0 \Rightarrow \boldsymbol{P}_\pm = \pm \begin{pmatrix} \frac{2}{\sqrt{3}}\arccos(-J_z/J_x) \\ 0 \end{pmatrix}. \tag{D4}$$

Now, we expand $f(\boldsymbol{k})$ around the Fermi points:

$$f(\boldsymbol{P}_\pm + \boldsymbol{p}) = \boldsymbol{p}\cdot\nabla f(\boldsymbol{P}_\pm) = A_\pm p_x + B_\pm p_y, \tag{D5}$$

where we have defined:

$$A_\pm = \mp\frac{\sqrt{3}}{2}\sqrt{4J_x^2 - J_z^2}, \quad B_\pm = -\frac{3}{2}J_z. \tag{D6}$$

Expanding the Hamiltonian H_{latt} around the Fermi point yields:

$$H_{\text{latt}} = \sum_{\boldsymbol{p}} \begin{pmatrix} a_+^\dagger & b_+^\dagger \end{pmatrix} (A_+ \sigma^1 p_x - B_+ \sigma^2 p_y) \begin{pmatrix} a_+ \\ b_+ \end{pmatrix} + \sum_{\boldsymbol{p}} \begin{pmatrix} a_-^\dagger & b_-^\dagger \end{pmatrix} (A_- \sigma^1 p_x - B_- \sigma^2 p_y) \begin{pmatrix} a_- \\ b_- \end{pmatrix}. \quad (D7)$$

Defining the four spinor and the gamma matrices:

$$\psi_{\boldsymbol{p}} = \begin{pmatrix} a_+ \\ b_+ \\ b_- \\ a_- \end{pmatrix}, \quad \gamma^0 = \begin{pmatrix} 0 & -\mathbf{1} \\ \mathbf{1} & 0 \end{pmatrix}, \quad \gamma^i = \begin{pmatrix} 0 & \sigma^i \\ \sigma^i & 0 \end{pmatrix}, \quad (D8)$$

with $\sigma^i = (\sigma^1, \sigma^2)$ Pauli matrices. Then we find $H_{\text{latt}} = \int d^2x \, \psi^\dagger \, \tilde{h}(\boldsymbol{p}) \, \psi$ with the single particle Hamiltonian:

$$\tilde{h}(\boldsymbol{p}) = \frac{\sqrt{3}}{2} \sqrt{4J_x^2 - J_z^2} \gamma^0 \gamma^1 p_x + \frac{3}{2} J_z \gamma^0 \gamma^2 p_y. \quad (D9)$$

where, for convenience, we have flipped the orientation of the y axis, i.e. $p_y \to -p_y$. In order to ensure hermiticity of the full Hamiltonian, the momentum operator is defined as $p_i = -i(\overrightarrow{\partial}_i - \overleftarrow{\partial}_i)/2$. Thus, we find:

$$\tilde{h}(\boldsymbol{p}) = \frac{\sqrt{3}}{2} \sqrt{4J_x^2 - J_z^2} \gamma^0 \gamma^1 (-i\partial_x) + \frac{3}{2} J_z \gamma^0 \gamma^2 (-i\partial_y) + \frac{\sqrt{3}i}{2} \partial_x \left(\sqrt{4J_x^2 - J_z^2} \right) \gamma^0 \gamma^1 + \frac{3i}{2} \partial_y J_z \gamma^0 \gamma^2. \quad (D10)$$

We can now generalise this Hamiltonian by considering the couplings J_x and J_z as position dependent, varying slowly compared to the lattice spacing. Next, we add a bosonic self-interacting Hamiltonian $\mathcal{H}_{\text{boson}}$,

$$\mathcal{H}_{\text{boson}} = \frac{1}{24\pi G} (\alpha_z^\dagger - \alpha_z) \left(\sqrt{2} (\alpha_x^\dagger - \alpha_x) - \frac{1}{2} (\alpha_z^\dagger - \alpha_z) \right) + \frac{8\pi G \mu^2}{3} \left(\alpha_z^\dagger \alpha_z + \alpha_x^\dagger \alpha_x \right)$$
$$- \frac{256\pi^3 G^3 \mu^2}{3l^2} \alpha_z^\dagger \alpha_z \left(\alpha_x^\dagger \alpha_x - \frac{1}{2} \alpha_z^\dagger \alpha_z \right), \quad (D11)$$

where α_x and α_z are bosonic modes at the edges of the lattice that control the tunnelling of fermions in the x and in the z direction, respectively (see figure 2). The optical lattice Hamiltonian that we will consider is then:

$$H_{\text{latt}} = \int d^2x \left[\psi^\dagger \, \tilde{h}(\boldsymbol{p}) \, \psi + \mathcal{H}_{\text{boson}} \right]. \quad (D12)$$

In order to show that (D12) can be mapped to (C4), first we consider the following form of the couplings:

$$J_m = \Delta_m D_m \left(D_m + d_m^\dagger + d_m \right), \quad m = x, z. \quad (D13)$$

where the operators d_m satisfy the commutation relations:

$$[d_m(x), d_n^\dagger(y)] = \delta_{mn} \delta^{(2)}(x - y),$$
$$[d_m(x), d_n(y)] = 0 = [d_m^\dagger(x), d_n^\dagger(y)], \quad (D14)$$

Note that this is a continuum version of the commutation relations given below equation (16). By considering:

$$D_x = -\frac{l}{4\pi G}, \qquad \Delta_x = \frac{32\pi^2 G^2}{3l^3}, \qquad D_z = -\frac{\sqrt{2}l}{8\pi G}, \qquad \Delta_z = \frac{64\pi^2 G^2}{3l^3}, \quad (D15)$$

one finds that the different terms in $\tilde{h}(\boldsymbol{p})$ given in (D10) can be written in the form:

$$\frac{3}{2} J_z = \frac{1}{l} - \frac{4\sqrt{2}\pi G}{l^2} \left(d_z^\dagger + d_z \right), \quad \frac{\sqrt{3}}{2} \sqrt{4J_x^2 - J_z^2} \approx \frac{1}{l} - \frac{16\pi G}{3l^2} \left(d_x^\dagger + d_x \right) + \frac{4\sqrt{2}\pi G}{3l^2} \left(d_z^\dagger + d_z \right), \quad (D16)$$

where in the last equality we have used the approximation:

$$\left| \langle d_m^\dagger + d_m \rangle \right| \ll |D_m|, \quad (D17)$$

valid for bosonic states in the weak fluctuation regime. Finally, we consider the operator redefinition:

$$q_1 = \frac{2\sqrt{2}}{3}d_x - \frac{1}{3}d_z, \qquad q_2 = d_z, \tag{D18}$$

which satisfy the canonical commutation relations given in (C8). This transformation maps the single particle Hamiltonian $\tilde{h}(\boldsymbol{p})$, given (D10), into the corresponding Hamiltonian $h(\boldsymbol{p})$ describing fermions coupled to dreibein fluctuations given in (C12).

Now we turn our attention to the bosonic Hamiltonian (D11), where the operators α_m are defined as:

$$\alpha_m = D_m + d_m. \tag{D19}$$

In this case we reverse the procedure and show that, up to an irrelevant additive constant, the gravitational Hamiltonian $\mathcal{H}_{\mathrm{gr}}$ given in (C13) can be mapped to (D11). This can be directly shown by noticing that:

$$
\begin{aligned}
(d_m^\dagger - d_m)(d_n^\dagger - d_n) &= (\alpha_m^\dagger - \alpha_m)(\alpha_n^\dagger - \alpha_n), \\
(d_m^\dagger + d_m)(d_m^\dagger + d_m) &\approx \frac{\alpha_m^\dagger \alpha_m \alpha_n^\dagger \alpha_n}{D_m D_n} - \frac{D_m}{D_m}\alpha_n^\dagger \alpha_n - \frac{D_n}{D_m}\alpha_m^\dagger \alpha_m + D_m D_n,
\end{aligned}
\tag{D20}
$$

and using (D15) and (D18). Note that in the last relation we have used $\alpha_m^\dagger \alpha_m \approx D_m^2 + D_m(d_m^\dagger + d_m)$, which holds in the approximation (D17).

Appendix E. Optical lattice realisation of the gravitational Hamiltonan

In order to realise the bosonic Hamiltonian (18), we consider the Hamiltonian for bosonic atoms, described by a bosonic mode $\Phi(\mathbf{x})$, in an optical lattice potential V_0 and a slowly varying external trapping potential V_T:

$$H = \int \mathrm{d}^3 x\, \Phi^\dagger(\mathbf{x})\left[-\frac{\nabla^2}{2m} + V_0(\mathbf{x}) + V_T(\mathbf{x})\right]\Phi(\mathbf{x}) + \frac{2\pi a_s^2}{m}\int \mathrm{d}^3 x\, \Phi^\dagger(\mathbf{x})\Phi^\dagger(\mathbf{x})\Phi(\mathbf{x})\Phi(\mathbf{x}), \tag{E1}$$

where a_s is the s-wave scattering length and m is the mass of the atoms [65]. For single atoms the energy eigenstates are Bloch wave functions and an appropriate superposition of Bloch states yields a set of Wannier functions which are well localized on the individual lattice sites. Expanding the field operator in the Wannier basis $w(\mathbf{x})$ in the following way,

$$\Phi(\mathbf{x}) = \sum_i \alpha_i \phi_i(\mathbf{x}), \quad \phi_i(\mathbf{x}) = w(\mathbf{x} - \mathbf{x}_i), \quad [\alpha_i, \alpha_j^\dagger] = \delta_{ij} \tag{E2}$$

one finds the Bose–Hubbard Hamiltonian:

$$H = -\sum_{<ij>} t_{ij}\,\alpha_i^\dagger \alpha_j + \sum_{<ijkl>} U_{ijkl}\,\alpha_i^\dagger \alpha_j^\dagger \alpha_k \alpha_l, \tag{E3}$$

where $<\cdots>$ denotes summation only over nearest neighbours. In (E3) we have defined the overlap integrals:

$$
\begin{aligned}
t_{ij} &= \int \mathrm{d}^3 x\, \phi_i^*(\mathbf{x})\left(-\frac{\nabla^2}{2m} + V_0(\mathbf{x}) + V_T(\mathbf{x})\right)\phi_j(\mathbf{x}) \\
U_{ijkl} &= \frac{4\pi a_s^2}{m}\int \mathrm{d}^3 x\, \phi_i^*(\mathbf{x})\,\phi_j^*(\mathbf{x})\,\phi_k(\mathbf{x})\,\phi_l(\mathbf{x}),
\end{aligned}
\tag{E4}
$$

where t_{ij} represents the tunnelling couplings (or the hopping matrix elements), whereas U_{ijkl} stands for the strength of the on-site repulsion of two atoms. We arrange the modes to be defined on a diamond lattice with indices $i = (\boldsymbol{i}, m)$, $j = (\boldsymbol{j}, n)$, etc, as shown in figure 1. For particular values of t_{ij} and U_{ijkl}, e.g. by changing the laser intensity or employing Feshbach resonances that control the scattering length, it is possible to tune appropriately the couplings and reproduce the gravitational Hamiltonian (18).

ORCID iDs

Patricio Salgado-Rebolledo ● https://orcid.org/0000-0001-6832-6785
Jiannis K Pachos ● https://orcid.org/0000-0002-9775-4436

References

[1] Volovik G E 2022 Gravity from symmetry breaking phase transition *J. Low Temp. Phys.* **207** 127–37

[2] Diako D 2011 Towards lattice-regularized quantum gravity (arXiv:1109.0091 [hep-th])

[3] Girvin S M, MacDonald A H and Platzman P M 1985 Collective-excitation gap in the fractional quantum hall effect *Phys. Rev. Lett.* **54** 581–3

[4] Girvin S M, MacDonald A H and Platzman P M 1986 Magneto-roton theory of collective excitations in the fractional quantum hall effect *Phys. Rev.* B **33** 2481–94

[5] Golkar S, Xuan Nguyen D X, Roberts M M and Thanh Son D T 2016 Higher-spin theory of the magnetorotons *Phys. Rev. Lett.* **117** 216403

[6] Gromov A and Thanh Son D 2017 Bimetric theory of fractional quantum hall states *Phys. Rev. X* **7** 041032

[7] Bergshoeff E A, Rosseel J and Townsend P K 2018 Gravity and the spin-2 planar schrödinger equation *Phys. Rev. Lett.* **120** 141601

[8] Pinczuk A, Dennis B S, Pfeiffer L N and West K 1993 Observation of collective excitations in the fractional quantum hall effect *Phys. Rev. Lett.* **70** 3983–6

[9] Kang M, Pinczuk A, Dennis B S, Eriksson M A, Pfeiffer L N and West K W 2000 Inelastic light scattering by gap excitations of fractional quantum hall states at $1/3 \leqslant \nu \leqslant 2/3$ *Phys. Rev. Lett.* **84** 546–9

[10] Zhou Z-Y, Guo-Xian S, Halimeh J C, Ott R, Sun H, Hauke P, Yang B, Yuan Z-S, Berges Jurgen and Pan J-W 2021 Thermalization dynamics of a gauge theory on a quantum simulator (arXiv:2107.13563)

[11] Iorio A, Pais P, Elmashad I A, Ali A F, Faizal M and Abou-Salem L I 2018 Generalized Dirac structure beyond the linear regime in graphene *Int. J. Mod. Phys.* D **27** 1850080

[12] Ciappina M F, Iorio A, Pais P and Zampeli A 2020 Torsion in quantum field theory through time-loops on dirac materials *Phys. Rev.* D **101** 036021

[13] Boada O, Celi A, Latorre J I and Lewenstein M 2011 Dirac equation for cold atoms in artificial curved spacetimes *New J. Phys.* **13** 035002

[14] Farjami A, Horner M D, Self C N, Papić Z and Pachos J K 2020 Geometric description of the Kitaev honeycomb lattice model *Phys. Rev.* B **101** 245116

[15] Ignacio Cirac J, Maraner P and Pachos J K 2010 Cold atom simulation of interacting relativistic quantum field theories *Phys. Rev. Lett.* **105** 190403

[16] Achucarro A and Townsend P K 1986 A Chern-Simons action for three-dimensional anti-de sitter supergravity theories *Phys. Lett.* B **180** 89

[17] Witten E 1988 (2+1)-dimensional gravity as an exactly soluble system *Nucl. Phys.* B **311** 46

[18] Brown J D and Henneaux M 1986 Central charges in the canonical realization of asymptotic symmetries: an example from three-dimensional gravity *Commun. Math. Phys.* **104** 207–26

[19] Coussaert O, Henneaux M and van Driel P 1995 The Asymptotic dynamics of three-dimensional Einstein gravity with a negative cosmological constant *Class. Quantum Grav.* **12** 2961–6

[20] Strominger A 1998 Black hole entropy from near horizon microstates *J. High Energy Phys.* JHEP02(1998)009

[21] Barnich G and Compere G 2007 Classical central extension for asymptotic symmetries at null infinity in three spacetime dimensions *Class. Quantum Grav.* **24** F15–F23

[22] Babichev E, Marzola L, Raidal M, Schmidt-May A, Urban F, Veermäe H and von Strauss M 2016 Heavy spin-2 dark matter *J. Cosmol. Astropart. Phys* JCAP09(2016)016

[23] de Rham C, Gabadadze G and Tolley A J 2011 Resummation of massive gravity *Phys. Rev. Lett.* **106** 231101

[24] Deser S, Jackiw R, Templeton S 1982 Three-dimensional massive Ge theories *Phys. Rev. Lett.* **48** 975–8

[25] Bergshoeff E A, Hohm O and Townsend P K 2009 Massive gravity in three dimensions *Phys. Rev. Lett.* **102** 201301

[26] Bergshoeff E A, de Haan S, Hohm O, Merbis W and Townsend P K 2013 Zwei-Dreibein gravity: a two-frame-field model of 3D massive gravity *Phys. Rev. Lett.* **111** 111102
Bergshoeff E A, de Haan S, Hohm O, Merbis W and Townsend P K 2013 Zwei-Dreibein gravity: a two-frame-field model of 3D massive gravity *Phys. Rev. Lett.* **111** 259902 (erratum)

[27] Schreiber M, Hodgman S S, Bordia P, Lüschen H P, Fischer M H, Vosk R, Altman E, Schneider U and Bloch I 2015 Observation of many-body localization of interacting fermions in a quasirandom optical lattice *Science* **349** 842–5

[28] Kondov S S, McGehee W R, Xu W and DeMarco B 2015 Disorder-induced localization in a strongly correlated atomic hubbard gas *Phys. Rev. Lett.* **114** 083002

[29] White M, Pasienski M, McKay D, Zhou S Q, Ceperley D and DeMarco B 2009 Strongly interacting bosons in a disordered optical lattice *Phys. Rev. Lett.* **102** 055301

[30] Choi J-Y, Hild S, Zeiher J, Schauß P, Rubio-Abadal A, Yefsah T, Khemani V, Huse D A, Bloch I and Gross C 2016 Exploring the many-body localization transition in two dimensions *Science* **352** 1547–52

[31] Wintersperger K, Braun C, Ünal F N, Eckardt A, Liberto M D Goldman N, Bloch I and Aidelsburger M 2020 Realization of an anomalous floquet topological system with ultracold atoms *Nat. Phys.* **16** 1058–63

[32] Scherg S, Kohlert T, Sala P, Pollmann F, Madhusudhana B H, Bloch I and Aidelsburger M 2021 Observing non-ergodicity due to kinetic constraints in tilted fermi-hubbard chains *Nat. Commun.* **12** 1–8

[33] Schweizer C, Grusdt F, Berngruber M, Barbiero L, Demler E, Goldman N, Bloch I and Aidelsburger M 2019 Floquet approach to $\mathbb{Z}_2$ lattice ge theories with ultracold atoms in optical lattices *Nat. Phys.* **15** 1168–73

[34] Yang B, Sun H, Ott R, Wang H-Y, Zache T V, Halimeh J C, Yuan Z-S, Hauke P and Pan J-W 2020 Observation of ge invariance in a 71-site bose–hubbard quantum simulator *Nature* **587** 392–6

[35] Milsted A, Liu J, Preskill J and Vidal G 2020 Collisions of false-vacuum bubble walls in a quantum spin chain (arXiv:2012.07243)

[36] Mil A, Zache T V, Hegde A, Xia A, Bhatt R P, Oberthaler M K, Hauke P, Berges J and Jendrzejewski F 2020 A scalable realization of local u (1) ge invariance in cold atomic mixtures *Science* **367** 1128–30

[37] Buser A J, Gharibyan H, Hanada M, Honda M and Liu J 2021 Quantum simulation of ge theory via orbifold lattice *J. High Energy Phys.* JHEP09(2021)034

[38] Alba E, Fernandez-Gonzalvo X, Mur-Petit J, Pachos J K and Garcia-Ripoll J J 2011 Seeing topological order in time-of-flight measurements *Phys. Rev. Lett.* **107** 235301

[39] Hauke P, Lewenstein M and Eckardt A 2014 Tomography of band insulators from quench dynamics *Phys. Rev. Lett.* **113** 045303

[40] Atala M, Aidelsburger M, Barreiro J T, Abanin D, Kitagawa T, Demler E and Bloch I 2013 Direct measurement of the Zak phase in topological bloch bands *Nat. Phys.* **9** 795–800

[41] Fläschner N, Rem B S, Tarnowski M, Vogel D-S, Lühmann D-S, Sengstock K, Weitenberg C 2016 Experimental reconstruction of the berry curvature in a floquet bloch band *Science* **352** 1091–4

[42] Gross C and Bloch I 2017 Quantum simulations with ultracold atoms in optical lattices *Science* **357** 995–1001

[43] Zohar E, Cirac J I and Reznik B 2015 Quantum simulations of lattice gauge theories using ultracold atoms in optical lattices *Rep. Prog. Phys.* **79** 014401

[44] Roberts J L, Claussen N R, Burke J P, Greene C H, Cornell E A and Wieman C E 1998 Resonant magnetic field control of elastic scattering in cold ^{85}Rb *Phys. Rev. Lett.* **81** 5109–12

[45] Bhaseen M J, Silver A O, Hohenadler M and Simons B D 2009 Feshbach resonance in optical lattices and the quantum ising model *Phys. Rev. Lett.* **103** 265302

[46] Amato-Grill J, Jepsen N, Dimitrova I, Lunden W and Ketterle W 2019 Interaction spectroscopy of a two-component mott insulator *Phys. Rev. A* **99** 033612

[47] Hui H and Liu X-J 2020 Consistent theory of self-bound quantum droplets with bosonic pairing *Phys. Rev. Lett.* **125** 195302

[48] Howl R, Vedral V, Naik D, Christodoulou M, Rovelli C and Iyer A 2021 Non-gaussianity as a signature of a quantum theory of gravity *PRX Quantum* **2** 010325

[49] Matos G, Hallam A, Deger A, Papić Z and Pachos J 2021 Emergence of gaussianity in the thermodynamic limit of interacting fermions (arXiv:2107.06906)

[50] Golan O and Stern A 2018 Probing topological superconductors with emergent gravity *Phys. Rev. B* **98** 064503

[51] Dasgupta A and Loll R 2001 A proper time cure for the conformal sickness in quantum gravity *Nucl. Phys.* B **606** 357–79

[52] Fierz M and Pauli W E 1939 On relativistic wave equations for particles of arbitrary spin in an electromagnetic field *Proc. R. Soc.* A **173** 211–32

[53] Bergshoeff E A, Hohm O and Townsend P K 2009 More on massive 3D gravity *Phys. Rev. D* **79** 124042

[54] Visser M 1998 Mass for the graviton *Gen. Relativ. Gravit.* **30** 1717–28

[55] Becker C, Soltan-Panahi P, Kronjäger J, Dörscher S, Bongs K and Sengstock K 2010 Ultracold quantum gases in triangular optical lattices *New J. Phys.* **12** 065025

[56] Yamamoto R, Ozawa H, Nak D C, Nakamura I and Fukuhara T 2020 Single-site-resolved imaging of ultracold atoms in a triangular optical lattice *New J. Phys.* **22** 123028

[57] Truscott A G, Strecker K E, McAlexander W I, Partridge G B and Hulet R G 2001 Observation of fermi pressure in a gas of trapped atoms *Science* **291** 2570–2

[58] Akatsuka T, Takamoto M and Katori H 2008 Optical lattice clocks with non-interacting bosons and fermions *Nat. Phys.* **4** 954–9

[59] Sugawa S, Inaba K, Taie S, Yamazaki R, Yamashita M and Takahashi Y 2011 Interaction and filling-induced quantum phases of dual mott insulators of bosons and fermions *Nat. Phys.* **7** 642–8

[60] Tarruell L, Greif D, Uehlinger T, Jotzu G and Esslinger T 2012 Creating, moving and merging dirac points with a fermi gas in a tunable honeycomb lattice *Nature* **483** 302–5

[61] Duca L, Li T, Reitter M, Bloch I, Schleier-Smith M and Schneider U 2015 An aharo-bohm interferometer for determining bloch band topology *Science* **347** 288–92

[62] Li T, Duca L, Reitter M, Grusdt F, Demler E, Endres M, Schleier-Smith M, Bloch I and Schneider U 2016 Bloch state tomography using wilson lines *Science* **352** 1094–7

[63] Horvath M S J, Thomas R, Tiesinga E, Deb A B and Kjærgaard N 2017 Above-threshold scattering about a feshbach resonance for ultracold atoms in an optical collider *Nat. Commun.* **8** 1–9

[64] Landig R, Hruby L, Dogra N, Landini M, Mottl R, Donner T and Esslinger T 2016 Quantum phases from competing short-and long-range interactions in an optical lattice *Nature* **532** 476–9

[65] Jaksch D, Bruder C, Cirac J I, Gardiner C W and Zoller P 1998 Cold bosonic atoms in optical lattices *Phys. Rev. Lett.* **81** 3108–11